Screening Effects in Flow through Rough Channels

J. S. Andrade, Jr.,[1,2,3] A. D. Araújo,[1] M. Filoche,[2,3] and B. Sapoval[2,3]
[1]*Departamento de Física, Universidade Federal do Ceará, 60451-970 Fortaleza, Ceará, Brazil*
[2]*Centre de Mathématiques et de leurs Applications, Ecole Normale Supérieure de Cachan, 94235 Cachan, France*
[3]*Physique de la Matière Condensée, Ecole Polytechnique, CNRS, 91128 Palaiseau, France*
(Received 18 May 2006; published 11 May 2007)

A surprising similarity is found between the distribution of hydrodynamic stress on the wall of an irregular channel and the distribution of flux from a purely Laplacian field on the same geometry. This finding is a direct outcome of numerical simulations of the Navier-Stokes equations for flow at low Reynolds numbers in two-dimensional channels with rough walls presenting either deterministic or random self-similar geometries. For high Reynolds numbers, the distribution of wall stresses on deterministic and random fractal rough channels becomes substantially dependent on the microscopic details of the walls geometry. Finally, the effects on the flow behavior of the channel symmetry and aspect ratio are also investigated.

DOI: 10.1103/PhysRevLett.98.194101 PACS numbers: 05.45.Df, 41.20.Cv, 47.53.+n

Partial differential equations are basic in the mathematical formulation of physical problems. The Laplace equation, for example, is known for its relevance in many fields, namely, electrostatics, heat transport, heterogeneous catalysis, and electrochemistry. The aim of the present work is first to reveal a surprising analogy between the properties of the solutions of 2D Laplace and Navier-Stokes equations when flow at low Reynolds and proper boundary conditions are imposed on the *same geometry*. In a second step, we present results obtained at higher Reynolds numbers and for distinct types of surface geometry.

The situations we compare and find to be quantitatively similar are displayed in Fig. 1. Figure 1(a) pictures the simplest Laplacian problem, namely, that of a capacitor with a prefractal electrode. The complex feature here is the distribution of charge on the irregular electrode or, in mathematical terms, the distribution of the harmonic measure. The recent research on this field has been dedicated mainly to the application of Laplacian transport towards and across irregular interfaces [1–5]. The system depicted in Fig. 1(b) corresponds to Stokes flow in a symmetric rough channel with the same geometry as in Fig. 1(a). The hydrodynamic quantity which is found to be distributed similarly to the harmonic measure in Fig. 1(a) is the viscous stress along the channel boundary. To obtain the potential field for the problem in Fig. 1(a), one must compute the solution of the Laplace equation with a potential $V = 1$ on the counterelectrode and zero potential on the irregular electrode (Dirichlet boundary condition). From that, it is then possible to calculate the charge σ_L^i on each elementary unit i of the wall and its corresponding normalized counterpart $\phi_L^i \equiv \sigma_L^i / \sum \sigma_L^j$. As previously shown [6], the distribution of ϕ_L along the irregular electrode is strongly nonuniform as a consequence of *screening effects*. This is a typical situation where the deep regions of the irregular surface support only a very small fraction of the total charge, as opposed to the more exposed parts [4].

The hydrodynamic question posed here has been triggered by the idea that the design of flowing systems should also include the influence of the surface geometry as a possibility for optimal performance. For this, we investigate the flow in a duct of length L and width h whose delimiting walls are identical prefractal interfaces with the geometry of a deterministic square Koch curve (SKC) [6]. The mathematical description for the fluid mechanics in this channel is based on the Navier-Stokes and continuity equations for flow under steady state conditions [7]. The Reynolds number is defined here as $\mathrm{Re} \equiv \rho V h / \mu$, where ρ and μ are the density and the viscosity of the fluid, respectively, and V is the average velocity at the inlet. In

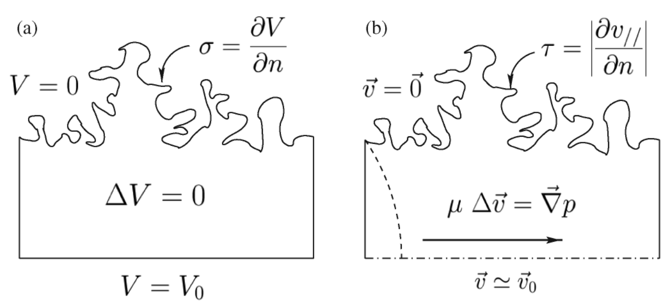

FIG. 1. The two different problems with similar solutions. In (a), we show a two-dimensional capacitor with an irregular electrode. The local charge is obtained from the numerical solution of the Laplace equation with Dirichlet boundary conditions. In (b), we see the analogous problem of flow at low Reynolds numbers. The rough channel is considered to be symmetrical with respect to the dotted-dashed line at the bottom. We consider nonslip boundary conditions at the entire solid-fluid interface, whereas a parabolic velocity profile is imposed at the inlet of the channel (the dashed curve). Here the stress parallel to the wall channel is calculated from the numerical solution of the continuity and Stokes (Re = 0) equations [7].

Fig. 2(a), we show the velocity vector field at low Re located at the self-similar reentrant zones that constitute the roughness of the irregular channel. Indeed, as depicted in Fig. 2(b), by rescaling the magnitude of the velocity vectors at the details of the roughness wall, we can observe fluid layers in the form of consecutive eddies. Although much less intense than the mainstream flow, these recirculating structures are located deeper in the system, being therefore strongly dependent on the landscape of the solid-fluid interface. More precisely, viscous momentum is transmitted laterally from the mainstream flow and across successive laminae of fluid to induce vortices inside the fractal cavity. These vortices will then generate other vortices of smaller sizes whose intensities fall off in geometric progression [8,9].

Once the velocity and pressure fields are obtained for the flow in the rough channel, we can compute the normalized stress ϕ_S^i at each elementary unit i of the wall $\phi_S^i \equiv \tau_S^i / \sum \tau_S^j$, where the sum is over the total number L_p of perimeter elements, the magnitude of the local stress is given by $\tau_S = |\partial v_\parallel / \partial n|$, the derivative is calculated at the wall element, $v_\parallel$ is the local component of the velocity that is parallel to the wall element, and n is the local normal coordinate. The semilog plot in Fig. 3(a) shows that the spatial distribution of normalized stresses at the interface is highly heterogeneous, with numerical values in a range that covers more than 5 orders of magnitude. Also shown in Fig. 3(a) is the variation along the interface of the normalized Laplacian fluxes ϕ_L crossing the wall elements of a Laplacian cell with Dirichlet boundary conditions. The astonishing similarity between these two distributions clearly suggests that the screening effect in flow could be reminiscent of the behavior of purely Laplacian systems. This is not totally unexpected, however, if we consider that the stream function of a Stokesian flow obeys the biharmonic equation. As shown in Fig. 3(b), this analogy is numerically confirmed through the very strong correlation between local stresses and Laplacian fluxes. These measures follow an approximately linear relationship, namely, $\phi_S \propto \phi_L$.

A further analogy can be drawn from the notion of *active zone* [1]. For two-dimensional Laplacian systems subjected to Dirichlet's boundary condition, the theorem of Makarov [2] essentially states that, whatever the shape (perimeter) of an interface, the size of the region where most of the activity takes place (the active zone) is of the order of the overall size L of the system. Here we define an *active length* as $L_a \equiv 1/\sum_{i=1}^{L_p} (\phi_S^i)^2$, with $1 \leq L_a \leq L_p$. If L_a is equal to the wall perimeter L_p, the entire wall works uniformly. However, the theorem of Makarov indicates that, for a purely Laplacian field, $L_a \approx L$. The results in Fig. 4(a) (open circles) show that the value of L_a for the square Koch curve remains approximately constant at $L_a/L = 0.55$ for low and moderate Reynolds numbers.

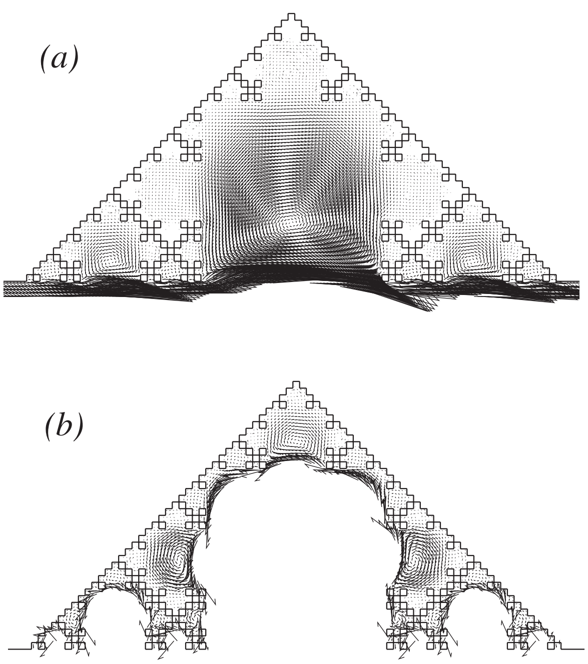

FIG. 2. (a) Vortices in the reentrant zones of the upper half of the (symmetric) prefractal roughness channel. The fluid flows steadily from left to right at a low Reynolds number Re = 0.01. (b) Sequence of the smaller eddies at the details of the roughness wall shown in (a).

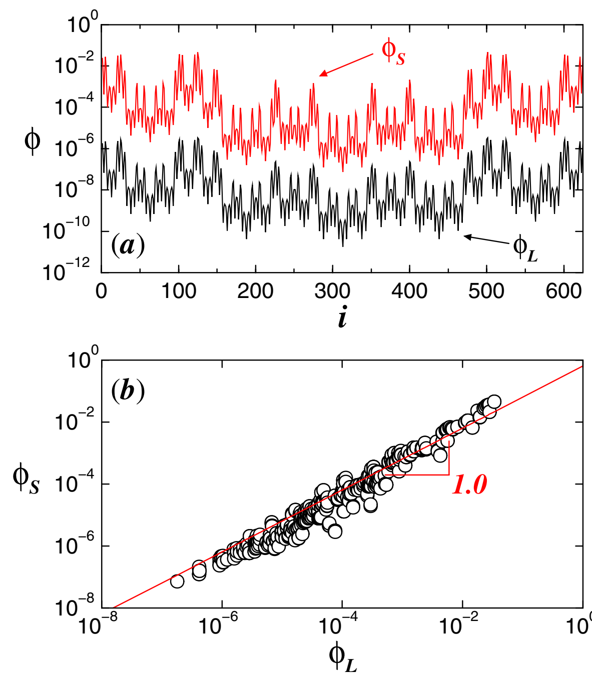

FIG. 3 (color online). (a) The dark (black) line is the curvilinear distribution of the logarithm of the normalized shear stresses ϕ_S on the interface along one of the two (symmetric) square Koch curves corresponding to the channel walls. The light (red) line gives the distribution of the logarithm of the normalized Laplacian charges ϕ_L for the analogous electrostatic problem. For better visualization, the distribution of ϕ_L has been shifted downwards. (b) Double-logarithmic plot of ϕ_S versus ϕ_L, with the red line indicating their linear relationship.

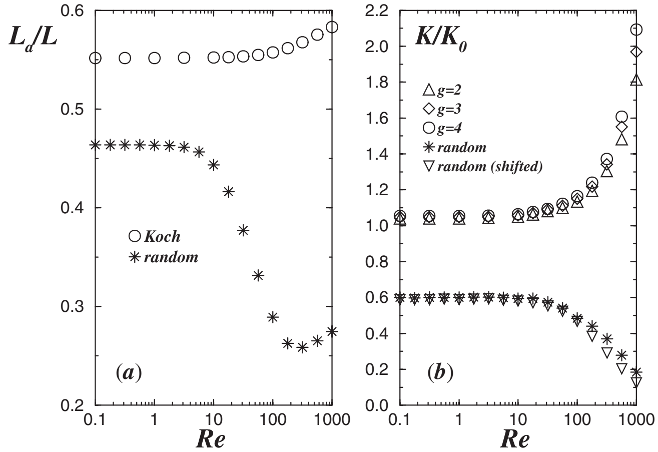

FIG. 4. (a) Semilog plot showing the dependence of the active length L_a on the Reynolds number Re for the (symmetrical) square Koch channel (empty circles) and random Koch channel (stars). The aspect ratio is $h/L = 1.0$. In (b), we show the semilog plot of the variation of the normalized permeability with Re for the random symmetrical (stars) and shifted (triangles down) Koch curves and the second (up triangles), third (diamonds), and fourth (circles) generations of the (symmetrical) square Koch channel.

This value is consistent with our screening analogy, because it indicates that the hydrodynamic stress is concentrated mainly on a subset of the wall whose size is of the order of the system size L. Only at higher Re values, when inertial forces become relevant, can one observe a small increase in L_a. The stress becomes slightly less localized due to the higher relative intensities of the vortices inside the deeper reentrant zones, when compared with the intensities of the correspondent flow structures at low Reynolds conditions.

The usual approach to describe single-phase fluid flow in irregular media (e.g., porous materials and fractures) is to characterize the system in terms of a macroscopic index, namely, the permeability K, which relates the average fluid velocity V with the pressure drop ΔP measured across the system $V = -K\Delta P/\mu L$. Figure 4(b) (open circles) shows that the permeability of the rough channel for low and moderate Re remains essentially constant at a value that is slightly above but very close to the reference permeability of a two-dimensional smooth channel, namely, ($K/K_0 \simeq 1$), with $K_0 \equiv h^2/12$ [10]. Above a transition point at Re $\simeq$ 10, the change in permeability reflects the onset of convective effects in the flow and, therefore, the sensitivity of the system to inertial nonlinearities. Surprisingly, one observes that, instead of decreasing with Re (i.e., a behavior that is typical of disordered porous media), the permeability of the SKC substantially increases. Moreover, as shown in Fig. 4(b), the higher the generation of the SKC, the higher is the permeability of the channel for a fixed value of Re above the transition. These results show that the screening effect of the hierarchical SKC geometry on the flow can be understood in terms of a reduction in the effective nonslip solid-fluid interface. In other words, we can imagine that each vortex present in a given generation of the SKC is, in fact, replacing one or a set of highly dissipative (nonslip) wall elements of SKCs of lower generations.

Next we study the fluid flow through a rough channel whose walls are composed of 10 successive and distinct realizations of the random Koch curve (RKC) of the third generation. Interestingly, the results shown in Fig. 4(a) (stars) indicate that the active length L_a of the wall stress calculated for the entire irregular interface geometry at low values of Re, $L_a/L \simeq 0.46$, is not substantially different from the SKC case, where $L_a/L = 0.55$. In Fig. 5, we show that the ratio L_a/L calculated individually for each of the 10 wall subsets composing the rough channel does not vary significantly from one unit to another. This is a rather unexpected behavior, especially if we consider the complexity of the different geometries involved (see Fig. 5). A similar effect has been observed for the purely Laplacian problem in a random geometry [5]. As depicted in Fig. 4(a), by increasing the Reynolds number, the departure from Stokes flow due to convection at Re $\simeq$ 10 results initially in the decrease of L_a/L (calculated over the entire surface) down to a minimum of approximately 0.25 at Re $\simeq$ 200. This behavior indicates the presence of long-range flow correlations imposed by inertia among successive wall subsets. More specifically, due to the randomness of these interface units, we can observe either "inward" (e.g., the wall subsets 2, 3, 4, 5, 6, and 8 in Fig. 5) or "outward" protuberances (e.g., the wall subsets 1, 7, 9, and 10 in Fig. 5) composing the roughness of the channel. Because of the symmetry of the system, the inward elements generate bottlenecks for flow. At high values of Re, the effect of inertia is to induce *flow separation lines* between the mainstream flow at the center of the channel and the flow near the wall, which can be as large as the largest distance between two consecutive bottlenecks. These exceedingly large "stagnation regions" are responsible for the initial decrease in the active length. If we increase the Reynolds

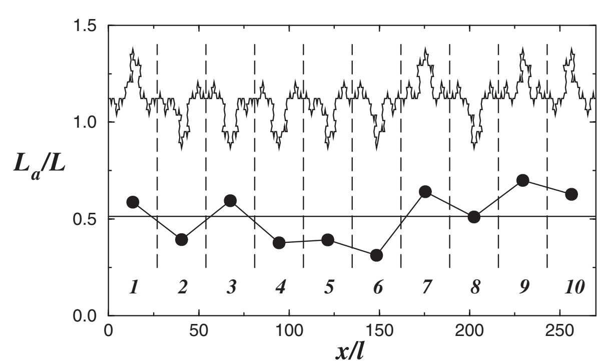

FIG. 5. The active length L_a for each of the 10 wall subsets composing the entire geometry of the (symmetrical) random Koch curve channel shown at the top. The dashed lines indicate the boundaries between consecutive subsets, as numbered below. The fluid flows from left to right at Re = 0.1.

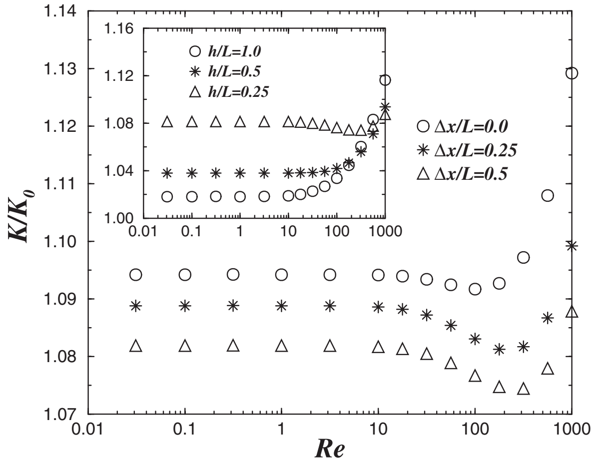

FIG. 6. Semilog plot of the normalized permeability against Re for flow in SKC channels generated with three different values of $\Delta x/L$ and an aspect ratio of $h/L = 0.25$. Here each wall interface is composed of three third-generation prefractal units. The inset reveals the effect of h/L on the curves K/K_0 versus Re for channels with walls shifted by $\Delta x/L = 0.5$.

number even more, the relative intensities of the vortices in these regions start to increase. As in the case of the SKC channel, L_a/L starts to increase due to a better distribution of shear stress near the wall.

In Fig. 4(b), we show the variation with Re of the permeability for the RKC channel (stars). In this case, we also observe a transition from linear (constant K) to nonlinear behavior that is typical of experiments with flow through real porous media and fractures [11]. Contrary to the results obtained for the SKC channel, however, the value of K calculated for low Re values is significantly different and smaller than the reference value K_0 of the corresponding smooth channel ($K/K_0 \simeq 0.6$). Once more, this is a consequence of the presence of several bottlenecks in the channel, which drastically reduce the effective space for flow. At high Reynolds, this difference is amplified due to inertial effects.

It is also important to understand the effect on the flow of the channel symmetry and aspect ratio h/L. Here the symmetry is broken by applying a longitudinal shift (x direction) of magnitude $\Delta x/L$ to one of the channel walls. In the case of the SKC channel, each wall interface is composed of three consecutive third-generation prefractal units. As shown in Fig. 6, the effect of the longitudinal shift is to generally decrease the permeability of the channel. By increasing $\Delta x/L$ for a small aspect ratio $h/L = 0.25$, we observe that a minimum in K/K_0 located right after the transition point Re $\simeq$ 10 becomes more pronounced. As a consequence, the original behavior observed in the symmetrical case, where the permeability tends to increase at higher Re numbers, is significantly attenuated. A similar tendency can be observed for the case of the RKC geometry [see Fig. 4(b)]. Compared to the symmetrical case, the presence of a longitudinal shift between the walls leads to a decrease in permeability at high Reynolds numbers. The results shown in the inset in Fig. 6 indicate that K/K_0 generally decreases with h/L. Moreover, the relative change in behavior between low and high Re numbers is substantially affected by this parameter. As previously observed, the permeability increases monotonically with Reynolds for $h/L = 1.0$ above the transition point Re $\simeq$ 10. While this behavior is still valid for $h/L = 0.5$, but in an attenuated form, a minimum in K/K_0 that is below the Darcy permeability level can be clearly observed for $h/L = 0.25$.

In summary, we have investigated the effect of deterministic and random roughness of 2D channels on local as well as macroscopic flow properties. At low Reynolds numbers, there exists a close analogy between the spatial distribution of the local stress on the rough walls and the distribution of charge resulting from the solutions of the Laplace equation in the same geometry. For a fractal deterministic roughness, a surprising increase of the permeability of symmetrical channels with Reynolds is observed. Moreover, this effect is augmented by increasing the fractal generation of the channel wall.

We thank the Brazilian agencies CNPq, CAPES, FUNCAP, and FINEP for financial support.

[1] B. Sapoval, Phys. Rev. Lett. **73**, 3314 (1994); B. Sapoval *et al.*, Chem. Eng. Sci. **56**, 5011 (2001).
[2] N. G. Makarov, Proc. London Math. Soc. **s3-51**, 369 (1985); P. Jones and T. Wolff, Acta Math. **161**, 131 (1988).
[3] P. Meakin *et al.*, Phys. Rev. A **32**, 2364 (1985); J. H. Kaufman *et al.*, Physica (Amsterdam) **157A**, 656 (1989).
[4] J. S. Andrade, Jr. *et al.*, Europhys. Lett. **55**, 573 (2001); Phys. Rev. E **68**, 041608 (2003); Physica (Amsterdam) **339A**, 296 (2004).
[5] M. Filoche and B. Sapoval, Phys. Rev. Lett. **84**, 5776 (2000).
[6] C. J. G. Evertsz and B. B. Mandelbrot, J. Phys. A **25**, 1781 (1992).
[7] S. V. Patankar, *Numerical Heat Transfer and Fluid Flow* (Hemisphere, Washington DC, 1980); we use the FLUENT fluid dynamics analysis package (FLUENT Inc.) in this study. The numerical solution for the velocity and pressure fields is obtained by means of the control volume finite-difference technique. For the fourth-generation SKC channel, a mesh of approximately a million elements generates satisfactory results when compared with numerical meshes of higher resolution.
[8] H. K. Moffat, J. Fluid Mech. **18**, 1 (1964).
[9] G. Leneweit and D. Auerbach, J. Fluid Mech. **387**, 129 (1999).
[10] R. B. Bird, W. E. Stewart and E. N. Lightfoot, *Transport Phenomena* (Wiley, New York, 1960).
[11] F. A. L. Dullien, *Porous Media - Fluid Transport and Pore Structure* (Academic, New York, 1979).